On the improvement of inelastic displacement demands for near-fault ground motions considering various faulting mechanisms

A. Esfahanian[a] and A.A. Aghakouchak[*]

*Faculty of Civil and Environmental Engineering, Tarbiat Modares University,
P.O. Box 11365-9313, Tehran, Iran*

Abstract. This paper investigates inelastic seismic demands of the normal component of near-fault pulse-like ground motions, which differ considerably from those of far-fault ground motions and also parallel component of near-fault ones. The results are utilized to improve the nonlinear static procedure (NSP) called Displacement Coefficient Method (DCM). 96 near-fault and 20 far-fault ground motions and the responses of various single degree of freedom (SDOF) systems constitute the dataset. Nonlinear Dynamic Analysis (NDA) is utilized as the benchmark for comparison with nonlinear static analysis results. Considerable influences of different faulting mechanisms are observed on inelastic seismic demands. The demands are functions of the strength ratio and also the pulse period to structural period ratio. Simple mathematical expressions are developed to consider the effects of near-fault motion and fault type on nonlinear responses. Modifications are presented for the DCM by introducing a near-fault modification factor, C_N. In locations, where the fault type is known, the modifications proposed in this paper help to obtain a more precise estimate of seismic demands in structures.

Keywords: forward directivity; pulse-like ground motion; near-fault earthquakes; nonlinear static procedure; displacement coefficient method; inelastic displacement ratio

1. Introduction

Performance-based engineering methods that rely on nonlinear static analysis procedures (NSP) for prediction of structural demands have been introduced in recent decades. FEMA 440 (2005) presents the results of a comprehensive study on this subject. This document reviews the related documents, namely FEMA 356 (2000) and ATC-40 (1996), and proposes improvements in calculating the inelastic displacement demand for a given ground motion. FEMA 440 includes descriptions of the two NSPs that were recommended by above-mentioned codes and used in practice. FEMA 356 utilized a displacement modification procedure (Displacement Coefficient Method), in which several empirically derived factors were used to modify the response of an

---

[*]Corresponding author, Professor, E-mail: a_agha@modares.ac.ir
[a]Ph.D. Candidate, E-mail: a.esfahanian@modares.ac.ir

elastic SDOF model of the structure to account for inelastic effects. The alternative Capacity-Spectrum Method (CSM) of ATC-40 used empirically derived relationships for the effective period and damping as a function of ductility to estimate the response of an equivalent linear SDOF oscillator in an iterative procedure. Recommendations of FEMA 440 have been implemented in some recent codes of practice such as ASCE41-06 (2007). Although many beneficial improvements have been presented for the displacement coefficient method and the capacity spectrum method in FEMA 440, but a review of the data used for this purpose shows that improvements consider far-fault (FF) ground motions mainly, and less data have been produced for near-fault (NF) earthquakes.

NF ground motions differ from FF ground motions in that they often contain strong coherent dynamic long period pulses and/or permanent ground displacements. Out of the two kinds of NF ground motions, i.e., pulse-like and non-pulse-like ground motions, ground motions with velocity pulses caused by near-fault directivity effects have received a great deal of attention because of their potential to cause severe damage to structures. In pulse-like NF ground motions, three outstanding characteristics are of interest: (1) ground motion is characterized by fault normal (FN) rotated record, which generally has larger amplitude than the fault parallel (FP), while non-pulse-like ground motions have equivalent FN and FP components; (2) FN pulse-like signals are characterized by a nonstandard pseudo acceleration spectral shape with an increment of spectral ordinates in a range around the pulse period (T_p), i.e., a bump shape; (3) inelastic to elastic displacement ratio for FN pulse-like records may virtually depart from the equal displacement rule, and can be higher than that of FF ground motions (Iervolino *et al.* 2012). Out of these three issues, the third one is related to inelastic seismic demand and is the focus of this paper.

NF ground motion with directivity or fling effects is significantly influenced by the rupture mechanism and is substantially different from FF records. This class of ground motion has large amplitude and long period, exhibits unusual response spectra shapes, possesses high *PGV/PGA* and *PGD/PGA* ratios and is best characterized in the velocity and the displacement time-histories. Such ground motion is also characterized by its energy being contained in a single or very few pulses, thus capable of causing severe damage to structures. Many of the buildings and bridges destroyed during the earthquake in Kobe (Japan 1995) are obvious instances for visualization of the effects of this kind of ground motions (Shaw and Goda 2004).

Many studies in recent years have investigated the dynamic response of structures to these pulse-like ground motions (Iervolino *et al.* 2012, Iwan *et al.* 2000, Baker 2007, Movahed *et al.* 2014), but the ground motions have usually been identified using judgment rather than some classification procedure. In order to identify pulse-like NF ground motions, a symmetric procedure was proposed by Baker (2007). This approach uses wavelet analysis to extract the largest velocity pulse from a given ground motion, which mostly occurs in the FN component of records. Three criteria described by Baker can then be combined to select the subset of pulse-like ground motions: (1) The pulse indicator (a function of *PGV* and energy ratio) is greater than 0.85, (2) The pulse arrives early in the time history, and (3) The original ground motion has a *PGV* of greater than 30 cm/sec.

It is well known that in addition to other factors such as earthquake magnitude, epicentral distance and soil type, the ground motions in a location are also a function of fault mechanism. Seismologists use the angle of the fault with respect to the surface (known as the dip) and the direction of slip along the fault to classify faults. They categorize faults into three main groups based on the sense of slip: a fault where the relative movement (or slip) on the fault plane is approximately vertical is known as a *dip-slip* fault (DS) where the slip is approximately horizontal,

the fault is known as a *strike-slip* (SS) fault and finally an *oblique-slip* (OS) or *combined* fault has non-zero components of both strike and dip slip. For all naming distinctions, it is the orientation of the net dip and sense of slip of the fault which must be considered, not the present-day orientation, which may have been altered by local or regional folding or tilting (Clough and Penzien 2003).

Based on above, this paper tries to suggest improvements for nonlinear static analysis procedures to accounts for the effects of NF pulse-like ground motions. The fault type influence on the inelastic response of structures is also studied. Improvements are presented for the current displacement coefficient method.

2. Review of the displacement coefficient method

In the displacement coefficient method, as presented in FEMA 356, the target displacement, δ_t, which corresponds to the displacement at roof level of a building, can be estimated using Eq. (1). In this equation, C_0 is the modification factor to relate spectral displacement of an equivalent SDOF system to the roof displacement of the MDOF system, C_1 is the modification factor to relate the expected maximum displacements of an inelastic SDOF oscillator with Elastic-Perfectly Plastic (EPP) hysteretic properties to displacements calculated for the linear elastic response, C_2 is the modification factor to represent the effect of pinched hysteretic shape, stiffness degradation, and strength deterioration on the maximum displacement response, and C_3 is the modification factor to represent increased displacements due to dynamic $P-\Delta$ effects (FEMA 356 2000)

$$\delta_t = C_0 C_1 C_2 C_3 S_a \frac{T_e^2}{4\pi^2} g \tag{1}$$

FEMA 440 recommends that the limitations (capping) imposed by FEMA 356 on the coefficient C_1 be abandoned. In addition, a distinction was recognized between two different types of strength degradation that have different effects on system response and performance, which led to recommendations for the coefficient C_2 to account for cyclic degradation in strength and stiffness. It was also suggested that the coefficient C_3 be eliminated and replaced with a limitation on strength. Although there have been some advantageous improvements for these coefficients in FEMA 440, no specific improvement was presented for the NF effects. In fact, their dataset included only 20 NF records with forward directivity and hence their effects were not separately investigated.

For a SDOF system, the inelastic to elastic displacement ratio, referred as C_μ or C_R in literature, is expressed as the maximum inelastic displacement demand, $\delta_{inelastic}$, divided by the maximum elastic displacement demand, $\delta_{elastic}$, for a system with the same properties, subjected to the same earthquake ground motion

$$C_R = \frac{\delta_{inelastic}}{\delta_{elastic}} \tag{2}$$

This coefficient is used as modification factor C_1 in FEMA, to relate expected maximum inelastic displacements to displacements calculated for linear elastic system.

Iwan *et al.* (2000) observed that for NF ground motions larger displacement amplification

factors and smaller strength reduction factors are indicated for structures having fundamental periods less than the predominant period of the ground motion, compared to far-field cases. Baez and Miranda (2000) found that displacement amplification factors are up to about 20% larger for near field sites, with fault normal amplifications being larger than fault parallel amplifications. MacRae and Tagawa (2001) recommended an R-μ-T relation for near field motions that change with directivity. Ruiz-Garcìa and Miranda (2006) investigated the inelastic displacement demands for structures built on soft soils and presented an analytical expression for the ratio of inelastic to elastic displacements for soft soils. They also developed inelastic displacement ratios (IDRs) for structures on firm sites (Miranda 2000). Baez and Miranda also studied amplification factors to estimate inelastic displacement demands for the design of structures in the near-field and concluded that IDRs corresponding to fault-normal components are, in general, larger than those of fault parallel components for periods between 0.1 and about 1.3 s (2000). From various parameters that may affect mean ratios of maximum inelastic displacement demand to maximum elastic displacement demand for structures located near active faults, it was found that peak ground velocity and maximum incremental velocity are the most important ones. Miranda also studied IDRs for displacement-based earthquake resistant design, and derived a simplified expression from nonlinear regression analyses in order to estimate mean IDRs of sites with average shear wave velocities higher than 180 m/sec. This expression is relatively simple and does not require the estimation of a site characteristic period (Miranda 2000). Later, Ruiz-Garcìa and Miranda supplemented the above-mentioned studies by evaluation of seismic displacement demands from ground motions recorded in recent earthquakes (2012). Enderami *et al.* proposed a new energy-based approach for predicting seismic demands of steel structures at the near-fault sites by introducing the concept of dissipated hysteretic input energy during largest yield excursion. They determined the peak global displacement demand on a different concept (2014).

Effect of soil-structure-interaction (SSI) on IDRs of existing structures was studied by Behmanesh and Khoshnudian (2008), in which, by developing a 4-DOF system, a parametric study was performed to investigate the effect of inertial SSI on inelastic displacement. They proposed a procedure, which appeared to be more accurate and easier to use in practice than the procedure proposed in FEMA440. Later, Khoshnudian *et al.* (2013) proposed a formula for predicting the IDRs of soil-structure systems. IDRs for SDOF structures subjected to repeated earthquakes was studied by Hatzigeorgiou and Beskos (2008) and a new method for evaluating the inelastic displacement ratios of SDOF systems on the basis of empirical expressions was obtained after extensive parametric studies. The influence of period of vibration, force reduction factor, soil type conditions, post-yield stiffness ratio (hardening and softening) and viscous damping ratio was deeply examined and discussed in this paper. Many studies investigated the functional form for prediction of NF pulse-like inelastic displacement ratio and derived analytical-form relationship for the inelastic displacement ratio. It was found that a double-opposite-bumps form is required to match the empirical data as a function of the structural period over the pulse period ratio. The relationship builds on previous studies on the topic, yet displays different shape with respect to the most common equations used for structural assessment procedures (Iervolino *et al.* 2012, Ruiz-Garcia 2011, Wen *et al.* 2014). Dimakopoulou *et al.* (2013) demonstrated how the seismic response varies with respect to the backbone parameters, the period and the seismic demand. The results show that the bilinear approximation, which is commonly used, underestimates the ductility demand compared to the quadrilinear case, regardless of the seismic intensity and the backbone parameters. Many other researchers also focused on this issue from different aspects (Akkar *et al.* 2004, Chioccarelli and Iervolino 2010, Ruiz-Garcìa 2011, Zhai *et al.* 2013, Decanini *et al.* 2003,

Ozkul *et al.* 2014, Ruiz-Garcìa and Gonzalez 2014), but they did not consider the fault type influence on inelastic displacement ratios in their studies.

3. Considered ground motions

In the past, mostly the strong ground motions within 30 km distance from faults were usually known as NF earthquakes. But nowadays, more precise procedures have been developed for categorizing NF records, especially for pulse-like ones. In this paper, wavelet analysis method, presented by Baker (2007, 2008) is used for selecting pulse-like NF ground motions. As mentioned in section 1, in this method three criteria are used to select the records, which can be considered as NF pulse-like ground motions. Those three conditions, in addition to the aforementioned limitation of 30 km distance from fault, seem to be a reasonable procedure in order to select suitable records.

Based on above, a set of 96 records (most of them identified earlier by Baker *et al.* 2007) from the NGA (Next Generation Attenuation project) database (http://peer.berkeley.edu/nga/) has been collected as listed in Table 1. Moment magnitude of records ranges from 5.0 to 7.6 and the vast majority of them are associated with C and D NEHRP site classification. On the other hand, for the purpose of verification and comparison, a set of 20 non-pulse-like (ordinary) records, all from type C soil condition, are also selected from the NGA database, as shown in Table 2. Datasets, in terms of number of records from each faulting mechanisms are summarized in Table 3.

Table 1 Recorded near-fault ground motions used in this study

#	Event	Year	Station	T_p[a]	PGA	PGV	M_w	Clo.D.[b] (km)	Epi. D.[c] (km)	Soil Type[d]	Fault Type[e]
1	San Fernando	1971	Pacoima Dam (upper left abut)	1.6	1.43451	116.5	6.6	1.8	11.9	B	Reverse
2	Coyote Lake	1979	Gilroy Array #6	1.2	0.45209	51.5	5.7	3.1	4.4	C	Strike-Slip
3	Imperial Valley-06	1979	Aeropuerto Mexicali	2.4	0.35735	44.3	6.5	0.3	2.5	C	Strike-Slip
4	Imperial Valley-06	1979	Agrarias	2.3	0.31146	54.4	6.5	0.7	2.6	C	Strike-Slip
5	Imperial Valley-06	1979	Brawley Airport	4.0	0.15803	36.1	6.5	10.4	43.2	C	Strike-Slip
6	Imperial Valley-06	1979	EC County Center FF	4.5	0.17972	54.5	6.5	7.3	29.1	C	Strike-Slip
7	Imperial Valley-06	1979	EC Meloland Overpass FF	3.3	0.37800	115.0	6.5	0.1	19.4	C	Strike-Slip
8	Imperial Valley-06	1979	El Centro Array #10	4.5	0.17611	46.9	6.5	6.2	26.3	C	Strike-Slip
9	Imperial Valley-06	1979	El Centro Array #11	7.4	0.37044	41.1	6.5	12.5	29.4	C	Strike-Slip
10	Imperial Valley-06	1979	El Centro Array #3	5.2	0.22925	41.1	6.5	12.9	28.7	C	Strike-Slip
11	Imperial Valley-06	1979	El Centro Array #4	4.6	0.35711	77.9	6.5	7.1	27.1	C	Strike-Slip
12	Imperial Valley-06	1979	El Centro Array #5	4.0	0.37540	91.5	6.5	4.0	27.8	C	Strike-Slip
13	Imperial Valley-06	1979	El Centro Array #6	3.8	0.44171	111.9	6.5	1.4	27.5	D	Strike-Slip
14	Imperial Valley-06	1979	El Centro Array #7	4.2	0.46239	108.8	6.5	0.6	27.6	C	Strike-Slip
15	Imperial Valley-06	1979	El Centro Array #8	5.4	0.46797	48.6	6.5	3.9	28.1	C	Strike-Slip
16	Imperial Valley-06	1979	El Centro Differential Array	5.9	0.41723	59.6	6.5	5.1	27.2	C	Strike-Slip

Table 1 Continued

#	Event	Year	Station	$T_p{}^a$	PGA	PGV	M_w	Clo.D.[b] (km)	Epi. D.[c] (km)	Soil Type[d]	Fault Type[e]
17	Imperial Valley-06	1979	Holtville Post Office	4.8	0.25809	55.1	6.5	7.7	19.8	C	Strike-Slip
18	Mammoth Lakes-06	1980	Long Valley Dam (Upr L Abut)	1.1	0.39891	33.1	5.9		14.0	C	Strike-Slip
19	Irpinia, Italy-01	1980	Sturno	3.1	0.23205	41.5	6.9	10.8	30.4	B	Normal
20	Westmorland	1981	Parachute Test Site	3.6	0.17195	35.8	5.9	16.7	20.5	C	Strike-Slip
21	Coalinga-05	1983	Oil City	0.7	0.86612	41.2	5.8		4.6	C	Reverse
22	Coalinga-05	1983	Transmitter Hill	0.9	0.85945	46.1	5.8		6.0	C	Reverse
23	Coalinga-07	1983	Coalinga-14th & Elm (Old CHP)	0.4	0.72883	36.1	5.2		9.6	C	Reverse
24	Morgan Hill	1984	Coyote Lake Dam (SW Abut)	1.0	0.81397	62.3	6.2	0.5	24.6	C	Strike-Slip
25	Morgan Hill	1984	Gilroy Array #6	1.2	0.24354	35.4	6.2	9.9	36.3	C	Strike-Slip
26	Taiwan SMART1(40)	1986	SMART1 C00	1.6	0.20499	31.2	6.3		68.2	B	Reverse
27	Taiwan SMART1(40)	1986	SMART1 M07	1.6	0.22946	36.1	6.3		67.2	B	Reverse
28	N. Palm Springs	1986	North Palm Springs	1.4	0.66966	73.6	6.1	4.0	10.6	D	Reverse-Oblique
29	San Salvador	1986	Geotech Investig Center	0.9	0.84561	62.3	5.8	6.3	7.9	C	Strike-Slip
30	Whittier Narrows-01	1987	Downey - Co Maint Bldg	0.8	0.23414	30.4	6.0	20.8	16.0	C	Reverse-Oblique
31	Whittier Narrows-01	1987	LB - Orange Ave	1.0	0.25543	32.9	6.0	24.5	20.7	C	Reverse-Oblique
32	Superstition Hills-02	1987	Parachute Test Site	2.3	0.41855	106.8	6.5	1.0	16.0	C	Strike-Slip
33	Loma Prieta	1989	Alameda Naval Air Stn Hanger	2.0	0.22221	32.2	6.9	71.0	90.8	C	Reverse-Oblique
34	Loma Prieta	1989	Gilroy Array #2	1.7	0.40619	45.7	6.9	11.1	29.8	C	Reverse-Oblique
35	Loma Prieta	1989	Oakland - Outer Harbor Wharf	1.8	0.33321	49.2	6.9	74.3	94.0	C	Reverse-Oblique
36	Loma Prieta	1989	Saratoga - Aloha Ave	4.5	0.36265	55.6	6.9	8.5	27.2	C	Reverse-Oblique
37	Erzican, Turkey	1992	Erzincan	2.7	0.48639	95.4	6.7	4.4	9.0	D	Strike-Slip
38	Cape Mendocino	1992	Petrolia	3.0	0.61481	82.1	7.0	8.2	4.5	C	Reverse
39	Landers	1992	Barstow	8.9	0.13817	30.4	7.3	34.9	94.8	C	Strike-Slip
40	Landers	1992	Lucerne	5.1	0.71000	140.3	7.3	2.2	44.0	C	Strike-Slip
41	Landers	1992	Yermo Fire Station	7.5	0.22176	53.2	7.3	23.6	86.0	C	Strike-Slip
42	Northridge-01	1994	Jensen Filter Plant	3.5	0.51781	67.4	6.7	5.4	13.0	B	Reverse
43	Northridge-01	1994	Jensen Filter Plant Generator	3.5	0.51788	67.4	6.7	5.4	13.0	C	Reverse
44	Northridge-01	1994	LA - Wadsworth VA Hospital North	2.4	0.27368	32.4	6.7	23.6	19.6	C	Reverse
45	Northridge-01	1994	LA Dam	1.7	0.57637	77.1	6.7	5.9	11.8	C	Reverse
46	Northridge-01	1994	Newhall - W Pico Canyon Rd.	2.4	0.42565	87.8	6.7	5.5	21.6	C	Reverse
47	Northridge-01	1994	Pacoima Dam (downstr)	0.5	0.49859	50.4	6.7	7.0	20.4	A	Reverse

Table 1 Continued

#	Event	Year	Station	$T_p{}^a$	PGA	PGV	M_w	Clo.D.[b] (km)	Epi. D.[c] (km)	Soil Type[d]	Fault Type[e]
48	Northridge-01	1994	Pacoima Dam (upper left)	0.9	1.37631	107.1	6.7	7.0	20.4	A	Reverse
49	Northridge-01	1994	Rinaldi Receiving Sta	1.2	0.86981	167.2	6.7	6.5	10.9	C	Reverse
50	Northridge-01	1994	Sylmar - Converter Sta	3.5	0.59429	130.3	6.7	5.4	13.1	C	Reverse
51	Northridge-01	1994	Sylmar - Converter Sta East	3.5	0.83871	116.6	6.7	5.2	13.6	C	Reverse
52	Northridge-01	1994	Sylmar - Olive View Med FF	3.1	0.73261	122.7	6.7	5.3	16.8	C	Reverse
53	Kobe, Japan	1995	Takarazuka	1.4	0.64523	72.6	6.9	0.3	38.6	D	Strike-Slip
54	Kobe, Japan	1995	Takatori	1.6	0.68200	169.6	6.9	1.5	13.1	D	Strike-Slip
55	Kocaeli, Turkey	1999	Gebze	5.9	0.23829	52.0	7.5	10.9	47.0	B	Strike-Slip
56	Chi-Chi, Taiwan	1999	CHY006	2.6	0.31149	64.7	7.6	9.8	40.5	C	Reverse-Oblique
57	Chi-Chi, Taiwan	1999	CHY035	1.4	0.26116	42.0	7.6	12.7	43.9	C	Reverse-Oblique
58	Chi-Chi, Taiwan	1999	CHY101	4.8	0.45133	85.4	7.6	10.0	32.0	D	Reverse-Oblique
59	Chi-Chi, Taiwan	1999	TAP003	3.4	0.09121	33.0	7.6	102.4	151.7	C	Reverse-Oblique
60	Chi-Chi, Taiwan	1999	TCU029	6.4	0.22069	62.3	7.6	28.1	79.2	C	Reverse-Oblique
61	Chi-Chi, Taiwan	1999	TCU031	6.2	0.11284	59.9	7.6	30.2	80.1	C	Reverse-Oblique
62	Chi-Chi, Taiwan	1999	TCU034	8.6	0.23108	42.8	7.6	35.7	87.9	C	Reverse-Oblique
63	Chi-Chi, Taiwan	1999	TCU036	5.4	0.13461	62.4	7.6	19.8	67.8	D	Reverse-Oblique
64	Chi-Chi, Taiwan	1999	TCU038	7.0	0.14082	50.9	7.6	25.4	73.1	C	Reverse-Oblique
65	Chi-Chi, Taiwan	1999	TCU040	6.3	0.14523	53.0	7.6	22.1	69.0	C	Reverse-Oblique
66	Chi-Chi, Taiwan	1999	TCU042	9.1	0.20944	47.3	7.6	26.3	78.4	C	Reverse-Oblique
67	Chi-Chi, Taiwan	1999	TCU046	8.6	0.14028	44.0	7.6	16.7	68.9	C	Reverse-Oblique
68	Chi-Chi, Taiwan	1999	TCU049	11.8	0.28105	44.8	7.6	3.8	38.9	C	Reverse-Oblique
69	Chi-Chi, Taiwan	1999	TCU053	12.9	0.22472	41.9	7.6	6.0	41.2	C	Reverse-Oblique
70	Chi-Chi, Taiwan	1999	TCU054	10.5	0.16888	60.9	7.6	5.3	37.6	C	Reverse-Oblique
71	Chi-Chi, Taiwan	1999	TCU056	12.9	0.12736	43.5	7.6	10.5	39.7	C	Reverse-Oblique
72	Chi-Chi, Taiwan	1999	TCU060	12.0	0.21026	33.7	7.6	8.5	45.4	D	Reverse-Oblique
73	Chi-Chi, Taiwan	1999	TCU065	5.7	0.82179	127.7	7.6	0.6	26.7	D	Reverse-Oblique
74	Chi-Chi, Taiwan	1999	TCU068	12.2	0.56207	191.1	7.6	0.3	47.9	C	Reverse-Oblique

Table 1 Continued

#	Event	Year	Station	T_p^a	PGA	PGV	M_w	Clo.D.[b] (km)	Epi. D.[c] (km)	Soil Type[d]	Fault Type[e]
75	Chi-Chi, Taiwan	1999	TCU075	5.1	0.33306	88.4	7.6	0.9	20.7	C	Reverse-Oblique
76	Chi-Chi, Taiwan	1999	TCU076	4.0	0.30459	63.7	7.6	2.8	16.0	C	Reverse-Oblique
77	Chi-Chi, Taiwan	1999	TCU082	9.2	0.24891	56.1	7.6	5.2	36.2	C	Reverse-Oblique
78	Chi-Chi, Taiwan	1999	TCU087	9.0	0.09917	53.7	7.6	7.0	55.6	C	Reverse-Oblique
79	Chi-Chi, Taiwan	1999	TCU098	7.5	0.10737	32.7	7.6	47.7	99.7	C	Reverse-Oblique
80	Chi-Chi, Taiwan	1999	TCU101	10.0	0.21779	68.4	7.6	2.1	45.1	C	Reverse-Oblique
81	Chi-Chi, Taiwan	1999	TCU102	9.7	0.29304	106.6	7.6	1.5	45.6	C	Reverse-Oblique
82	Chi-Chi, Taiwan	1999	TCU103	8.3	0.13233	62.2	7.6	6.1	52.4	C	Reverse-Oblique
83	Chi-Chi, Taiwan	1999	TCU104	12.0	0.11052	31.4	7.6	12.9	49.3	C	Reverse-Oblique
84	Chi-Chi, Taiwan	1999	TCU128	9.0	0.18741	78.7	7.6	13.2	63.3	C	Reverse-Oblique
85	Chi-Chi, Taiwan	1999	TCU136	10.3	0.16945	51.8	7.6	8.3	48.8	C	Reverse-Oblique
86	Northwest China-03	1997	Jiashi	1.3	0.26627	37.0	6.1		19.1	B	Strike-Slip ?
87	Yountville	2000	Napa Fire Station #3	0.7	0.60056	43.0	5.0		9.9	D	Strike-Slip
88	Chi-Chi, Taiwan-03	1999	CHY024	3.2	0.18680	33.1	6.2	19.7	25.5	C	Reverse
89	Chi-Chi, Taiwan-03	1999	CHY080	1.4	0.47318	69.9	6.2	22.4	29.5	C	Reverse
90	Chi-Chi, Taiwan-03	1999	TCU076	0.9	0.52418	59.4	6.2	14.7	20.8	C	Reverse
91	Chi-Chi, Taiwan-06	1999	CHY101	2.8	0.12631	36.3	6.3	36.0	50.0	D	Reverse
92	Tabas, Iran	1978	Tabas	6.1	0.85176	121.2	7.4	1.8	13.9	B	Reverse
93	Bam, Iran	2003	Bam	1.7	0.79906	101.5	6.6	10	45	B	Strike-Slip
94	Kocaeli, Turkey	1999	Yarimca	4.4	0.34899	62.2	7.5	1.4	4.8	C	Strike-Slip
95	Kocaeli, Turkey	1999	Arcelik	6.8	0.14990	39.6	7.5	10.6	13.5	C	Strike-Slip
96	Cape Mendocino	1992	Cape Mendocino	4.8	1.49731	125.5	7.0	7.0	4.5	C	Reverse

[a]Pulse period of the eartquake record, [b]Closest distance to fault, [c]Epicentral distance of faults, [d]From NEHRP site class, [e]Faulting mechanism

Table 2 Recorded far-fault ground motions on soil type C used in this study

#	Event	Year	Station	PGA	M_w	Closest D.	Epi. D.	Soil Type	Fault Type
1	Loma Prieta	1989	Yerba Buena Island	0.06780	7.1	75.1	75.2	C	Reverse-Oblique
2	Loma Prieta	1989	APEEL 7, Pulgas	0.15646	7.1	41.7	41.9	C	Reverse-Oblique
3	Loma Prieta	1989	Anderson Dam, Downstream	0.24386	7.1	19.9	20.3	C	Reverse-Oblique
4	Northridge	1994	Castaic, Old Ridge Route	0.51426	6.8	20.1	20.7	C	Reverse
5	Northridge	1994	Littlerock, Brainard Canyon	0.07202	6.8	46.3	46.6	C	Reverse

Table 2 Continued

#	Event	Year	Station	PGA	M_w	Closest D.	Epi. D.	Soil Type	Fault Type
6	N. Palm Springs	1986	Fun Valley	0.12865	6.0	12.8	14.2	C	Reverse-Oblique
7	San Fernando	1971	Pearblossom Pump	0.13575	6.5	35.5	39	C	Reverse
8	Imperial Valley	1979	El Centro, Parachute Test Site	0.20382	6.8	12.7	12.7	C	Strike-Slip
9	Northridge	1994	Lake Hughes #1, Fire station #78	0.08660	6.8	35.5	35.8	C	Reverse
10	Loma Prieta	1989	Monterey, City Hall	0.07278	7.1	39.7	44.4	C	Reverse-Oblique
11	Caldiran, Turkey	1976	Maku	0.09748	7.2	50.8	50.8	C	Strike-Slip?
12	Chi-Chi, Taiwan	1999	CHY041	0.30192	7.6	19.4	19.8	C	Reverse-Oblique
13	Cape Mendocino	1992	Shelter Cove Airport	0.22851	7.0	26.5	28.8	C	Reverse
14	Cape Mendocino	1992	Eureka - Myrtle & West	0.17821	7.0	40.2	42	C	Reverse
15	Upland	1990	Rancho Cucamonga - FF	0.24023	5.6	10.9	11	C	Strike-Slip
16	Kocaeli, Turkey	1999	Hava Alani	0.09007	7.5	58.3	60	C	Strike-Slip
17	Norcia, Italy	1979	Spoleto	0.03903	5.9	13.3	13.4	C	Normal
18	Norcia, Italy	1979	Cascia	0.016129	5.9	1.7	4.6	C	Normal
19	Kocaeli, Turkey	1999	Goynak	0.11873	7.5	31.7	31.7	C	Strike-Slip
20	Hector Mine	1999	Hector	0.26558	7.1	10.3	11.7	C	Strike-Slip

Forward directivity results when the fault rupture propagates toward the site at a velocity nearly equal to the propagation velocity of the shear waves and it eventually produces velocity pulses. But it should be noted that not all identified pulses are from directivity effects. The period of detected velocity pulse (T_p), a parameter of interest in NF ground motions, is easily determined by velocity response spectra and more precisely by wavelet algorithm. Table 4 shows the distribution of pulse-like records in different T_p bins. The distribution of velocity pulses for each faulting mechanisms is also illustrated in Fig. 1, which shows the scattering of T_p for each fault type. It can be seen that OS faults cover wider range of T_p, in comparison to SS and DS faults, which have narrower scattering range in T_p, respectively.

Obviously the pulse period (Tp) is not known for earthquakes before their occurrence. But it is a significant parameter in estimating inelastic demands using the formulae proposed later in the

Table 3 Pulse-like and ordinary datasets

Mechanism	Records	Pulse-like records	ordinary records
Strike-slip	40	34	6
Dip-slip (Reverse & Normal)	33	25	8
Oblique-slip (Combined)	47	37	6
Total	116	96	20

Table 4 Distribution of pulse-like records in T_p bins

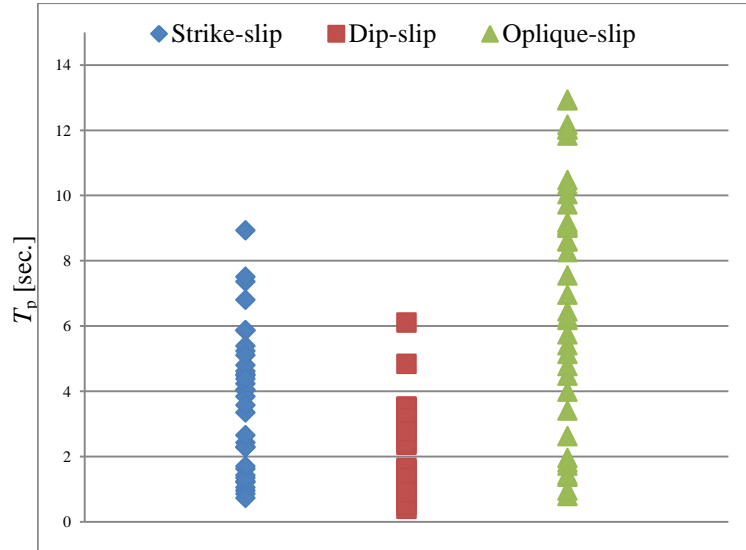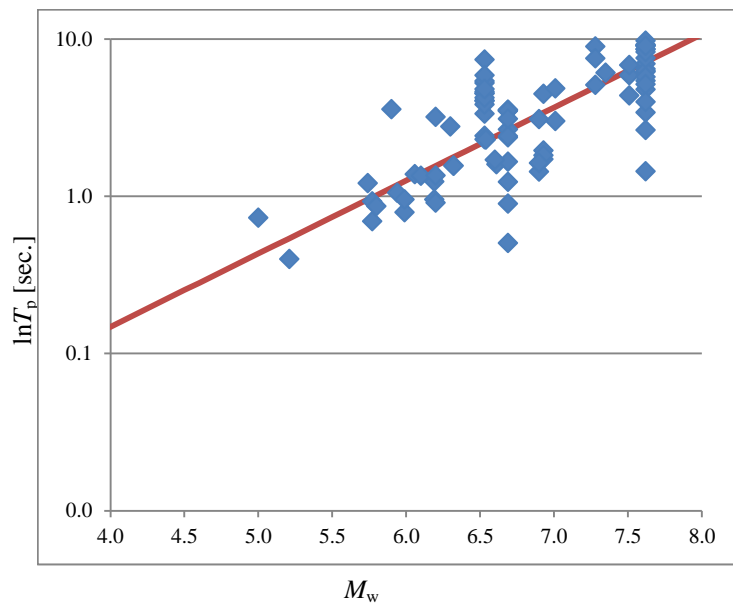| T_p	[0, 1s]	[1, 2s]	[2, 3s]	[3, 4s]	[4, 5s]	[5, 6s]	[6, 12s]
Number of records	9	17	8	11	11	8	32

Fig. 1 Scattering of T_p values for each faulting mechanisms

Fig. 2 Comparison between extracted pulse periods and predicted values by regression of NGA data

paper. Therefore the data presented in this section may help to predict the T_p value merely by estimating the moment magnitude (M_w) of a fault under consideration with the Gutenberg-Richter or similar laws in the absence of the time-history of the record.

It has already been observed that the period of any resulting velocity pulse is related primarily to the earthquake magnitude (Shahi and Baker 2011). In order to confirm correct identification of pulse-like records, a comparison was carried out with respect to NGA records. The extracted T_p values were compared with the expected pulse period calculated from Eq. (3), which is based on a

Table 5 Regression results for various faulting mechanisms

	Strike-slip	Dip-slip	Oblique-slip
a	-4.756	-6.571	-5.809
b	0.894	1.111	1.306

regression analysis of the NGA record dataset (Chioccarelli and Iervolino 2010).This equation gives the natural logarithm of T_p as a function of M_w. The comparison is illustrated in Fig. 2, in which a good agreement is observed

$$\ln T_p = -6.19 + 1.07.M_W \tag{3}$$

Similarly, separate equations are presented here for various faulting mechanisms by the same format ($\ln T_p = a + bM_W$), which are demonstrated in Table 5. These equations result in direct estimation of pulse period from earthquake moment magnitude. Hence, by predicting the moment magnitude for a fault under consideration, the pulse period may be estimated quickly.

4. Inelastic displacement ratio (IDR)

Nonlinear Dynamic Analysis (NDA) is considered as 'exact' method, however, it is very time-consuming and may not be suitable for everyday engineering practice, which favors the use of NSP in engineering practice as an alternative method (FEMA 273 1997). Therefore, NDA is considered the benchmark for verifying nonlinear static analysis results. In this work NDA has been carried out for a variety of SDOF systems, when subjected to: (a) sets of NF pulse-like records; (b) a set of ordinary ground motions. The SDOF systems were designed to cover practical range of periods of vibration and different levels of nonlinearity. Periods of vibration ranged from T=0.1 s to T=3 s. These periods were selected by an increment of 0.1s from T=0 to T=1, an increment of 0.2s from T=1 to T=2, and an increment of 0.5s from T=2 to T=3. Nonlinearity level is measured by means of strength ratio R. This ratio represents the ratio of elastic strength demand to yield strength of a structural system and is defined by Eq. (4), as a function of elastic spectral acceleration for 5% damping, $S_a(T_o, 5\%)$, and the natural period of structure, m the mass of the SDOF system, and F_y the yielding strength. In this work R=2, 3, 4, 5 and 6 were considered

$$R = \frac{m.S_a(T_o)}{F_y} \tag{4}$$

It should be noted that all of the considered ground motions in this study are used in their unscaled form, because the yield strength of the SDOF systems were adjusted in the way that the desired strength ratio, R, be attained.

EPP hysteretic model was considered here in this study. After carrying out time-history analysis for the linear and nonlinear systems, the inelastic to elastic displacement ratio, C_R, were determined. It must be mentioned that in FEMA 440 four different hysteretic behaviors are introduced, including the elastic perfectly plastic (EPP), stiffness-degrading (SD), strength and stiffness-degrading (SSD), and nonlinear elastic (NE) models. From these four models, the EPP

model is used as a reference model. This model has been used widely in previous investigations and therefore it represents a benchmark to study the effect of hysteretic behavior. Furthermore, recent studies have shown that this is a reasonable hysteretic model for steel beams that do not experience lateral or local buckling or connection failure. The SD model is representative of well detailed and flexuraly controlled reinforced concrete structures in which the lateral stiffness decreases as the level of lateral displacement increases. The SSD model can reproduce the response of poorly detailed reinforced concrete structures relatively well. The NE model approximately reproduces the behavior of pure rocking structures. Therefore, although EPP model does not always represent the realistic behavior of structures, it is used as a reference model in this paper for the considered SDOF systems to study the effects of NF ground motions.

Therefore, a total of 9,806 IDRs were computed corresponding to 116 ground motions, 17 periods of vibration, and 5 levels of strength ratio. Mean IDRs were then computed for each period and each strength ratio, the results of which will be presented hereafter.

Several studies have revealed that pulse-like motions in FN direction (Chioccarelli and Iervolino 2010) are generally stronger than both fault parallel components and non-pulse-like ground motions; yet, not enough is known about the probable influence of fault type on nonlinear response of structures. As explained previously in section 1, faults are categorized in three sets, namely SS, DS and OS types. As shown in Table 3, in this study 34 records are SS type, 25 records are DS type and the remaining 37 records are OS type. Results of NDAs in this study are illustrated in Fig. 3, which shows mean IDRs of SDOF systems versus the periods of vibration for strength ratios of 2, 3, 4, 5 and 6, corresponding to all FF and NF ground motions, regardless of their faulting mechanism.

The differences of IDRs for the two types of ground motion are clear in Fig. 3. The equal displacement rule is applicable for periods of vibration more than 1.3 s in FF records and for periods more than about 3 s in NF records. From Fig. 3(a), it can be seen that mean IDRs are characterized by being larger than 1 in the short-period spectral region, but they reach about 1 for periods longer than about 3.0 s. For periods smaller than 2.0 s, IDRs are strongly dependent on the period of vibration and on the level of nonlinearity. In general, in this spectral region maximum
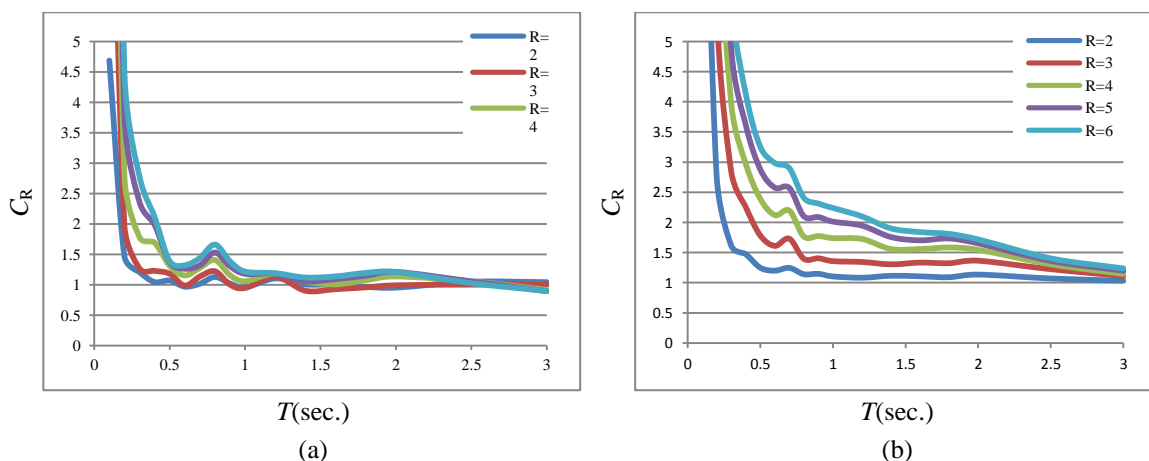

Fig. 3 Mean inelastic displacement ratios for different R values vs. period for: (a) All FF ground motions, (b) All NF ground motions

inelastic displacements become much larger than maximum elastic displacements as the strength ratio increases and as the period decreases. It is noteworthy that there are obvious bumps, representing a peak in C_R for period of about 0.6 s for all R values. Besides, the C_R coefficient for NF ground motions is observed to be at least 50 percent higher compared to that of FF ground motions in the considered period range. Also, these differences become more pronounced by increasing the nonlinearity level and decreasing the period. Therefore, the inefficiency of utilizing C_R of FF records for NF ones is obvious and some modifications are needed in order to use this coefficient for NF ground motions. It means that the C_1 coefficient of FEMA 440 is not capable of predicting the nonlinear response of structures subjected to NF earthquakes correctly. Now in order to study the influence of faulting mechanism on the seismic demands, the data obtained for NF ground motions are divided into three sets and the variations of C_R are shown in Fig. 4.

In Figs. 4(a), (b), (c), considerable differences are obvious for various faulting mechanisms which demonstrate the fact that the fault type can have considerable influences on nonlinear
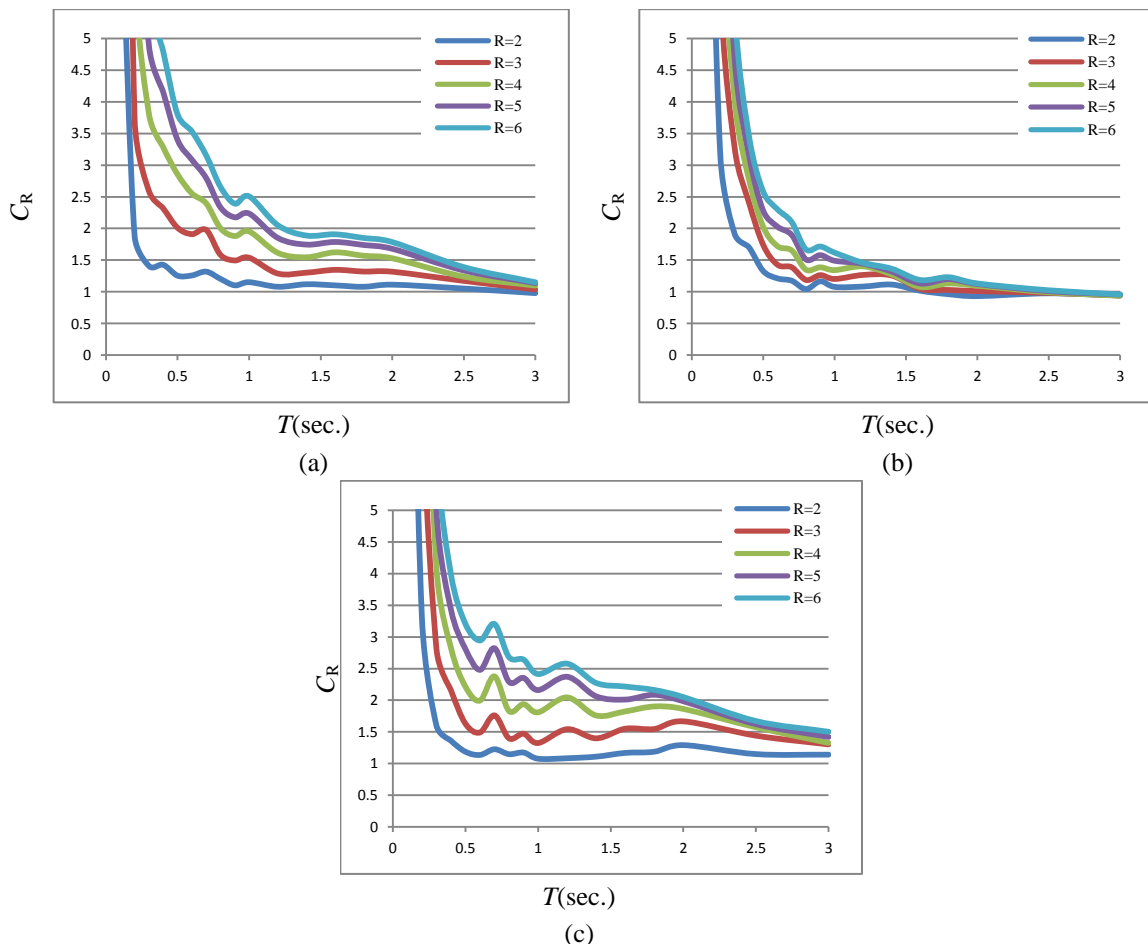
Fig. 4 Mean Inelastic Displacement Ratios for different R values vs. period for: (a) SS fault type NF Ground Motions, (b) DS fault type, (c) OS fault type

response of structure. OS faults seem to create larger demands compared to SS and DS faults.

Ma and Archuleta (2006) studied the mechanism dependence of radiated seismic energy from three hypothetical crustal events by modeling spontaneous ruptures. They concluded that the reverse fault has the largest apparent stress compared to that of the strike-slip fault and normal fault. Therefore, the discussion on T_p values presented in section 3 also conforms this trend. It means that T_p is somehow representative of fault's radiated seismic energy and the larger the value of T_p, the higher C_R values would be. Therefore, in order to reduce the scatters in results of Figs. 3-4 and also for better comparison, periods of vibration were normalized with respect to the pulse period, shown in Table 2, and the results are represented in Fig. 5. This method is vastly used in most of the similar researches in the literature and also in FEMA 440.

Furthermore, Shahi and Baker (2011) showed that the period of the pulse primarily depends on the magnitude of the earthquake in all fault types, but the closest distance to the fault and the V_{s30} also had an influence on the pulse period in case of strike-slip earthquakes. Therefore, the faulting mechanism directly affects the value of the pulse period (T_p).

In order to show the dispersion of the C_R Parameter considering different faulting mechanisms (Fig. 5), the Coefficient of Variation (CV), also known as relative variability, is utilized. This
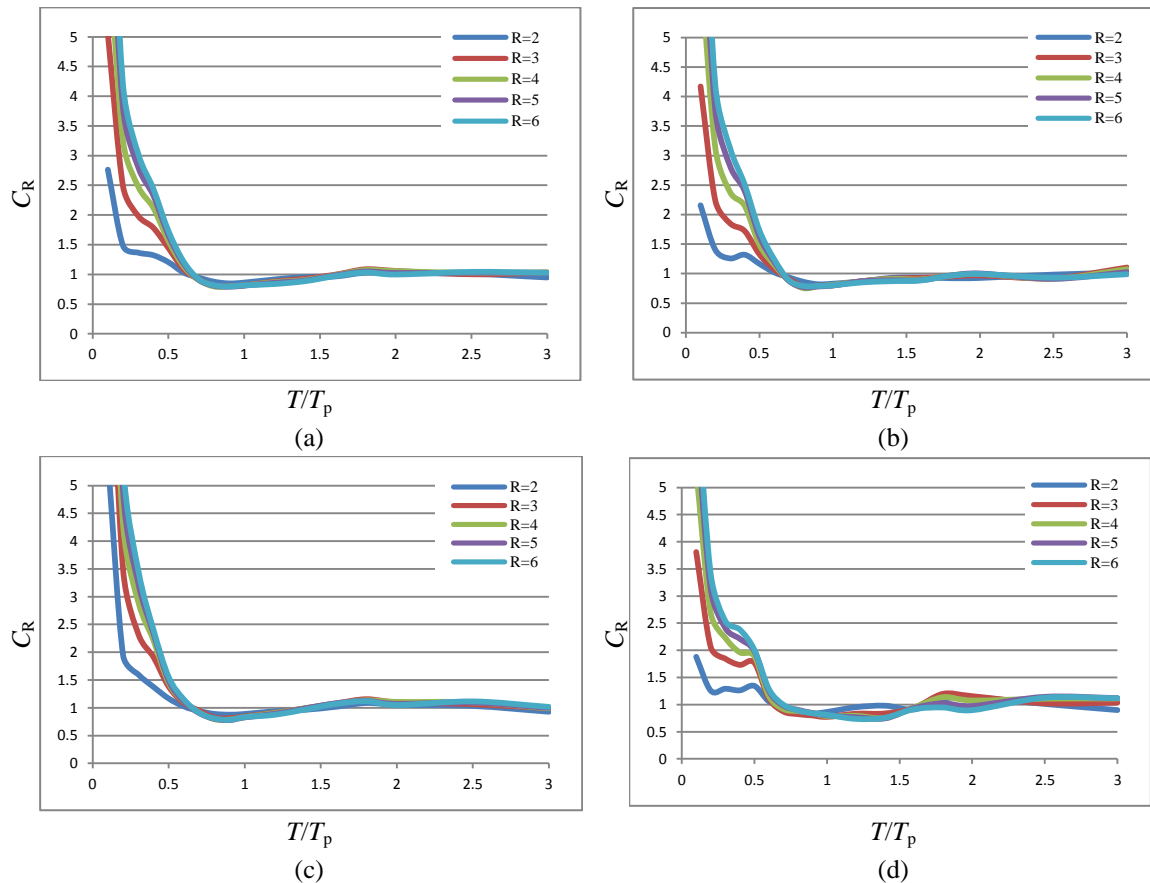

Fig. 5 Mean inelastic displacement ratios for different R values vs. normalized period for: (a) All NF ground motions, (b) SS fault type NF ground motions, (c) DS fault type, (d) OS fault type

parameter represents the ratio of the standard deviation to the mean, and it is a useful statistic for indicating the degree of variation from one data series to another. The lower the CV, the smaller the residuals are relative to the predicted value.

The CV is calculated for all fault types, as illustrated in Fig. 6. The results show that for low values of T/T_p there are large variations but for higher values of this parameter CVs are approximately 0.2.

From Fig. 5(a), for NF ground motions the equal displacement rule is applicable for T/T_p longer than about 0.6 for all strength ratios, regardless of the faulting mechanism. For smaller values of T/T_p, the equal displacement rule is not applicable as displacements ratios vary by R. Figs. 5(b), (c), (d), show similar pattern for different fault types, except for OS faults, for which this point differs slightly and reaches about 0.65. In OS faults IDRs are dependent on the period of vibration and on the level of nonlinearity for all T/T_p ranges, especially in low T/T_p range (i.e., values less than 0.65).

For a better investigation of this effect, the results were once again normalized for each set with respect to the average of all fault types. Figs. 7(a), (b), (c) show mean inelastic displacement
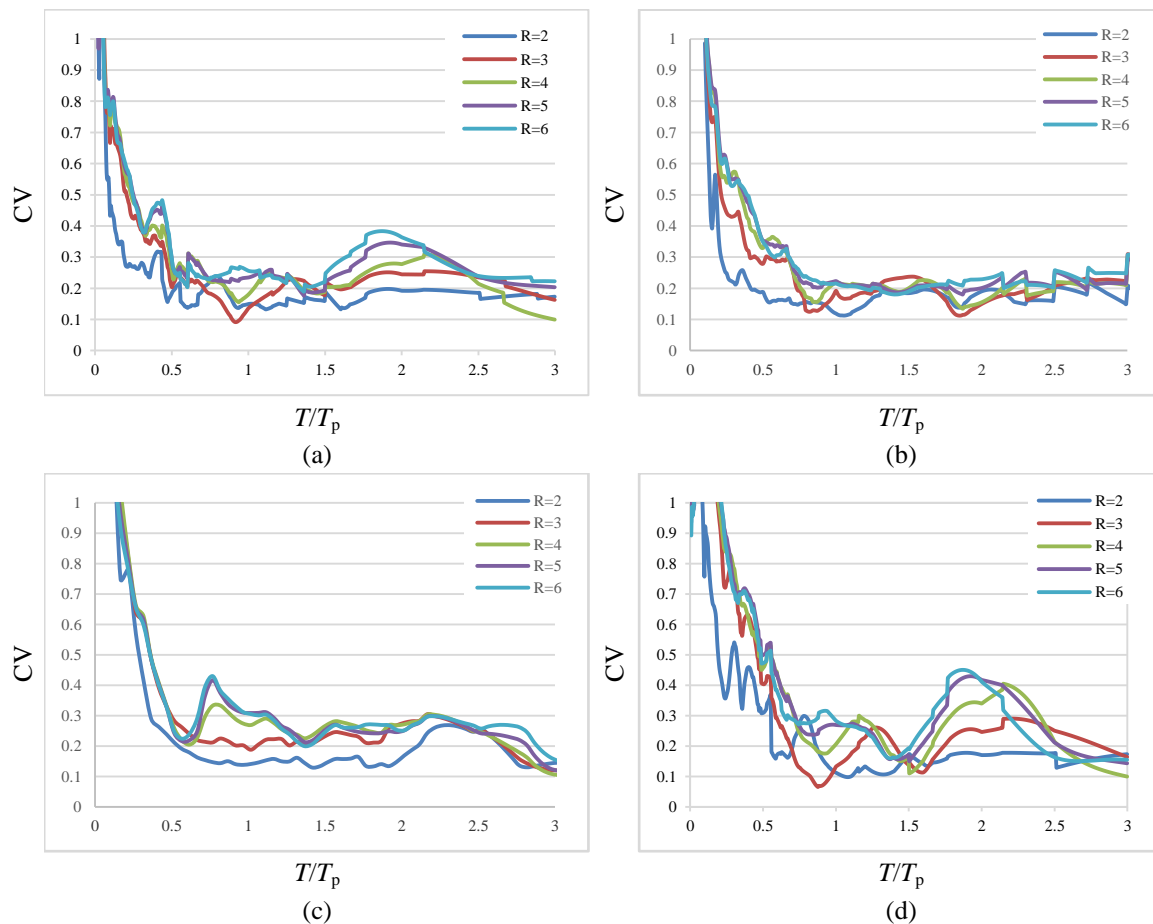

Fig. 6 Coefficient of variations of C_R values for NF ground motions: (a) All NF ground motions, (b) SS fault type NF ground motions, (c) DS fault type, (d) OS fault type
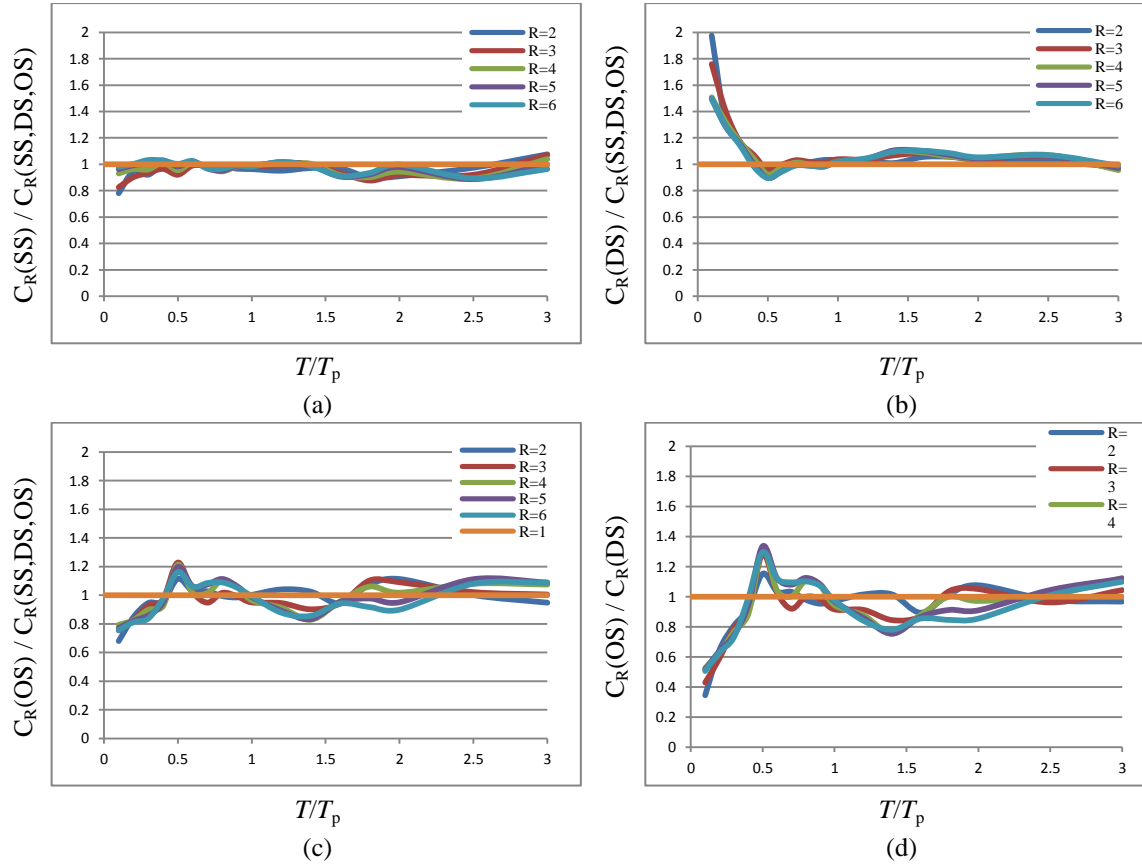
Fig. 7 Mean inelastic displacement ratios on each group normalized by mean ratios from all ground motions: (a) SS type faults; (b) DS type faults; (c) OS type faults; (d) OS to DS type faults

ratios for fault types SS, DS, and OS, respectively. It can be seen that for SS faults, normalized mean inelastic displacement ratios are, in general, slightly smaller than 1 and they fluctuate about 1. Thus, for these faults neglecting the effect of faulting mechanism on C_R would result in a small overestimation of inelastic displacement demands. For DS faults normalized mean inelastic displacement ratios are slightly larger than 1 in the whole T/T_p range, except for $0.3<T/T_p<0.7$ range. For $T/T_p<0.3$, the results are larger and an average C_R would result in large underestimation of inelastic displacement demands. For OS faults normalized mean inelastic displacement ratios have considerable fluctuations around 1 and are highly dependent on R and T/T_p. These variations lead to about 20% underestimation and nearly 20% overestimation in the considered range. For $T/T_p=0.6$, the results grow larger and an average C_R would result in large underestimation of inelastic displacement demands. As a comparison, the mean C_R values for the strongest mechanism (OS) were then divided by the weakest one (SS) and the results are illustrated in Fig. 7(d).

5. Regression analysis

The results presented in previous section show that inelastic to elastic displacement ratio, C_R,

for pulse-like NF ground motions are not compatible with those of FF ones. Therefore, the C_1 coefficient presented in FEMA 440may not be capable of covering pulse-like NF ground motions. This coefficient seems to be only applicable for FF (i.e., ordinary earthquakes) or FP component of NF earthquakes. In FEMA 440, the inelastic to elastic spectral response displacement coefficient, C_1, is given by the relationship in Eq. (5), where α accounts for site soil conditions; i.e., the constant α is equal to 130, 90, and 60 for site classes B, C, and D, respectively

$$C_1 = 1 + (R-1)/(\alpha.T^2)$$ (5)

Therefore, for application to NF ground motions, a modification should be carried out on C_1, which is done here in the form of a modification factor, C_N. By multiplying this factor by C_1, results would take into account the NF effects.

In order to achieve this goal, the C_1 coefficients of FEMA 440 were calculated for each inelastic SDOF system and they were compared with NDA. The modification factor, C_N, is then defined as follows

$$(C_N)_{T,R} = \left[\frac{(C_R)_{ex}}{(C_1)_{app}}\right]_{T,R}$$ (6)

Fig. 8 shows samples of the values of C_1, C_R and C_N for R=2 and R=4. It should be noted that this figure is for the whole NF ground motions not considering fault types. It is observed that C_1 coefficient of FEMA 440 underestimates the NF ground motion responses in T/T_p<0.6 range and it overestimates the results in 0.6<T/T_p<2.0 range. For T/T_p>2.0, both C_1 and C_R give the same results and NF effects could be neglected and no specific modification is needed in this range. In other words, the equal displacement rule is satisfied for T/T_p>2.0.

Having created such data for all levels of nonlinearity it was tried to derive a parametric equation describing C_N using nonlinear regression analysis (Levenberg-Marquardt algorithm) in
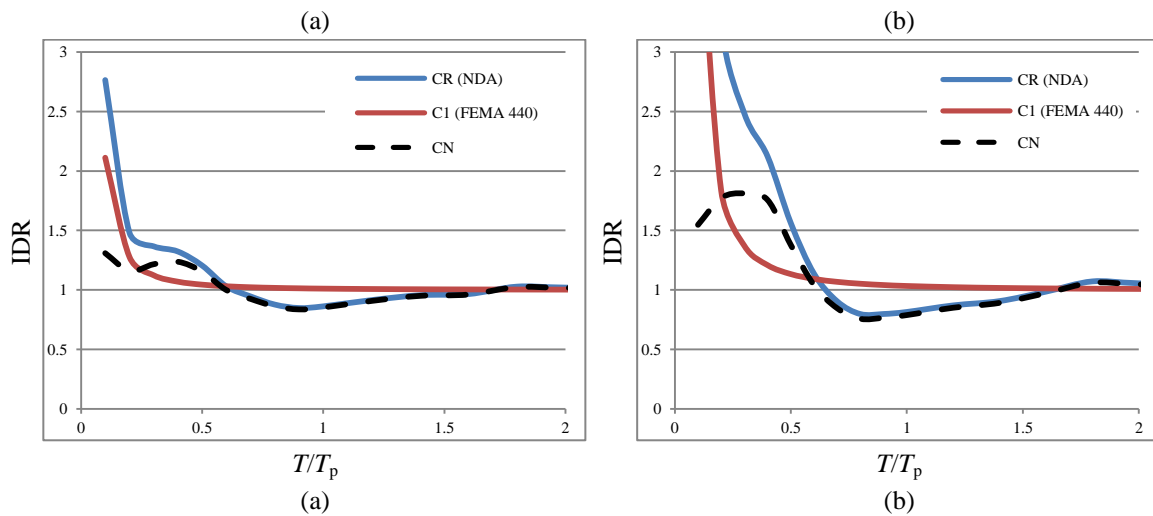
(a)

(b)

(a)

(b)

Fig. 8 Extracting C_N by comparing C_1 of FEMA 440 and C_R for NF coefficients: (a) R=2; (b) R=4

order to determine the coefficients of Eq. (7). In this equation, the influences of faulting mechanism may also be considered. The polynomial functions of order 4 and 5 have been able to estimate the C_N coefficient for $T/T_p<0.6$ and $0.6< T/T_p<2.0$, respectively

$$
C_N = \begin{cases} \theta_1 \cdot \left(\dfrac{T}{T_p}\right)^4 + \theta_2 \cdot \left(\dfrac{T}{T_p}\right)^3 + \theta_3 \cdot \left(\dfrac{T}{T_p}\right)^2 + \theta_4 \left(\dfrac{T}{T_p}\right) + \theta_5 & \dfrac{T}{T_p} \le 0.6 \\[3ex] \theta_6 \cdot \left(\dfrac{T}{T_p}\right)^5 + \theta_7 \cdot \left(\dfrac{T}{T_p}\right)^4 + \theta_8 \left(\dfrac{T}{T_p}\right)^3 + \theta_9 \left(\dfrac{T}{T_p}\right)^2 + \theta_{10} \left(\dfrac{T}{T_p}\right) + \theta_{11} & 0.6 < \dfrac{T}{T_p} \le 2.0 \\[3ex] 1 & \dfrac{T}{T_p} > 2.0 \end{cases} \tag{7}
$$

Table 6 Coefficient estimates for Eq. (7) for all NF records

	R=2	R=3	R=4	R=5	R=6
θ_1	56.906	31.056	56.038	65.453	61.594
θ_2	-94.409	-50.151	-74.323	-84.355	-76.594
θ_3	52.397	23.072	25.042	26.468	20.604
θ_4	-11.439	-3.7251	1.1121	0.0929	1.9105
θ_5	2.0175	1.7586	1.4801	1.3118	1.0482
θ_6	-0.6166	-2.0747	-3.0002	-2.9062	-3.011
θ_7	4.5088	14.017	20.252	19.666	20.26
θ_8	-13.159	-37.378	-53.608	-52.28	-53.562
θ_9	19.09	49.282	69.609	68.293	69.622
θ_{10}	-13.515	-31.88	-44.089	-43.582	-44.274
θ_{11}	4.5492	8.8348	11.624	11.581	11.726

Table 7 Coefficient estimates for Eq. (7) for all NF records as functions of R

θ_i	Equation
θ_1	$2.862(R-1)^4 - 39.68(R-1)^3 + 191.9(R-1)^2 - 366.9(R-1) + 268.6$
θ_2	$-3.288(R-1)^4 + 46.64(R-1)^3 - 231.8(R-1)^2 + 462.6(R-1) - 368.5$
θ_3	$1.045(R-1)^4 - 15.76(R-1)^3 + 84.08(R-1)^2 - 186.9(R-1) + 169.9$
θ_4	$0.476(R-1)^3 - 5.545(R-1)^2 + 21.85(R-1) - 28.38$
θ_5	$0.007(R-1)^2 - 0.281(R-1) + 2.289$
θ_6	$0.2662(R-1)^2 - 2.1589(R-1) + 1.2274$
θ_7	$-1.7607(R-1)^2 + 14.279(R-1) - 7.7294$
θ_8	$4.5309(R-1)^2 - 36.756(R-1) + 18.431$
θ_9	$-5.6692(R-1)^2 + 46.023(R-1) - 20.528$
θ_{10}	$3.433(R-1)^2 - 27.92(R-1) + 10.529$
θ_{11}	$-0.7938(R-1)^2 + 6.4729(R-1) - 1.0236$

The goal is now to find constant factors θ_i (for i=1, 2, 3, 4, 5, 6, 7, 8, 9, 10, 11) that best fit the data. If all the NF data are considered, these constants are found as presented in Table 6. In this case, the error of using Eq. (7) is illustrated in Fig. 9(a). In this figure, the horizontal axis shows the actual analytical data and the vertical one demonstrates the approximate figures calculated from Eq. (7). This figure demonstrates good correspondence between actual modification factor and the estimated ones.

Once appropriate values for θ_i for different levels of R were found, it was tired to derive a relationship between θ_i and R in terms of polynomial functions. Table 7 presents these relationships for θ_i constants when all NF data were considered. Similar expressions were also derived considering various faulting mechanisms, which are shown in Table 8. The accuracy of these expressions was also examined and the results are presented in Figs. 9(b), (c), (d) for SS, DS, and OS fault types, respectively.
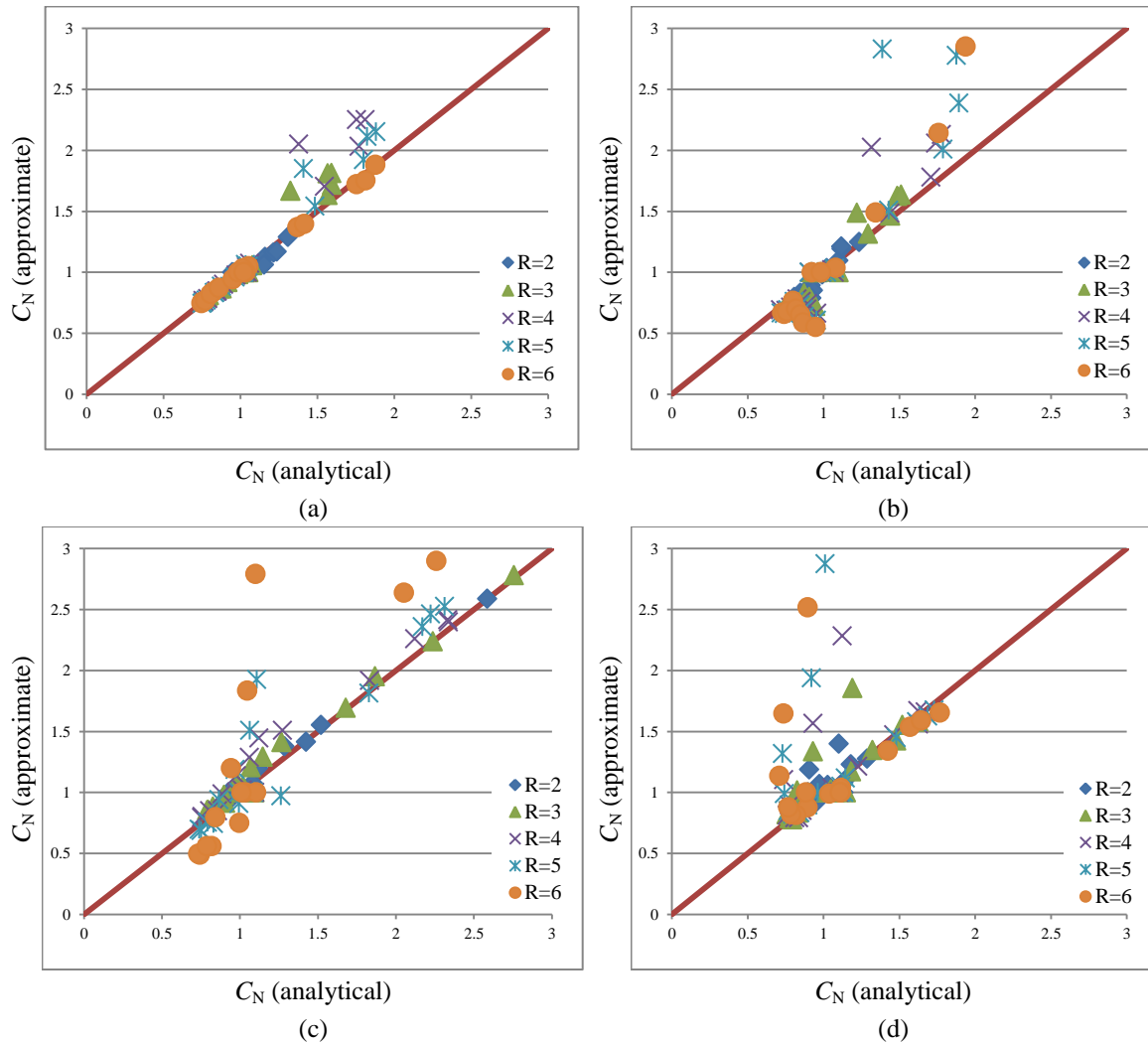

Fig. 9 Errors of curve-fitting: (a) All fault types; (b) SS type faults; (c) DS type faults; (d) OS type faults

Table 8 Coefficient estimates for Eq. (7) considering different faulting mechanisms as functions of *R*

θ_i	Equation
	Strike-slip faulting mechanism
θ_1	$50.94(R-1)^4 - 558.8(R-1)^3 + 2066(R-1)^2 - 2998(R-1) + 1454$
θ_2	$-59.77(R-1)^4 + 655.4(R-1)^3 - 2420(R-1)^2 + 3502(R-1) - 1705$
θ_3	$24.06(R-1)^4 - 263.5(R-1)^3 + 971.8(R-1)^2 - 1406(R-1) + 688.3$
θ_4	$-3.85(R-1)^4 + 42.08(R-1)^3 - 154.7(R-1)^2 + 224.3(R-1) - 109.9$
θ_5	$0.205(R-1)^4 - 2.238(R-1)^3 + 8.155(R-1)^2 - 11.49(R-1) + 6.487$
θ_6	$0.371(R-1)^2 - 3.477(R-1) + 4.134$
θ_7	$-2.551(R-1)^2 + 23.65(R-1) - 27.05$
θ_8	$6.781(R-1)^2 - 62.22(R-1) + 67.73$
θ_9	$-8.666(R-1)^2 + 78.76(R-1) - 80.58$
θ_{10}	$5.290(R-1)^2 - 47.73(R-1) + 45.22$
θ_{11}	$-1.220(R-1)^2 + 10.96(R-1) - 8.615$
	Dip-slip faulting mechanism
θ_1	$8.694(R-1)^4 - 117.2(R-1)^3 + 569.9(R-1)^2 - 1172(R-1) + 938.71$
θ_2	$-5.472(R-1)^4 + 90.66(R-1)^3 - 525.8(R-1)^2 + 1271(R-1) - 1191$
θ_3	$1.025(R-1)^4 - 24.19(R-1)^3 + 176.2(R-1)^2 - 516.2(R-1) + 567.4$
θ_4	$0.379(R-1)^4 - 2.466(R-1)^3 - 4.476(R-1)^2 + 57.45(R-1) - 100.7$
θ_5	$-0.096(R-1)^4 + 1.096(R-1)^3 - 3.932(R-1)^2 + 3.697(R-1) + 5.1$
θ_6	$-0.083(R-1)^4 + 0.956(R-1)^3 - 3.767(R-1)^2 + 5.774(R-1) - 4.182$
θ_7	$0.605(R-1)^4 - 7.011(R-1)^3 + 27.79(R-1)^2 - 42.60(R-1) + 29.8$
θ_8	$-1.669(R-1)^4 + 19.44(R-1)^3 - 77.18(R-1)^2 + 117.4(R-1) - 80.34$
θ_9	$2.161(R-1)^4 - 25.21(R-1)^3 + 99.76(R-1)^2 - 149.2(R-1) + 101.3$
θ_{10}	$-1.313(R-1)^4 + 15.28(R-1)^3 - 59.98(R-1)^2 + 87.46(R-1) - 59.69$
θ_{11}	$0.299(R-1)^4 - 3.462(R-1)^3 + 13.41(R-1)^2 - 18.90(R-1) + 14.05$
	Oblique-slip faulting mechanism
θ_1	$-4.898(R-1)^3 + 62(R-1)^2 - 227.5(R-1) + 121.3$
θ_2	$5.209(R-1)^3 - 70.27(R-1)^2 + 269.6(R-1) - 150.6$
θ_3	$-1.642(R-1)^3 + 25.36(R-1)^2 - 106.9(R-1) + 62.46$
θ_4	$0.135(R-1)^3 - 3.078(R-1)^2 + 16.01(R-1) - 8.718$
θ_5	$0.016(R-1)^3 - 0.111(R-1)^2 + 0.071(R-1) + 0.633$

Table 8 Continued

θ_i	Equation
θ_6	$-0.381(R-1)^3 + 4.126(R-1)^2 - 12.98(R-1) + 7.061$
θ_7	$2.428(R-1)^3 - 26.04(R-1)^2 + 81.00(R-1) - 42.27$
θ_8	$-5.961(R-1)^3 + 63.31(R-1)^2 - 194.3(R-1) + 96.26$
θ_9	$7.065(R-1)^3 - 74.22(R-1)^2 + 224.7(R-1) - 104.2$
θ_{10}	$-4.030(R-1)^3 + 41.9(R-1)^2 - 125.4(R-1) + 53.69$
θ_{11}	$0.871(R-1)^3 - 8.983(R-1)^2 + 26.66(R-1) - 9.39$

It must be recalled that Iervolino *et al.* (2012) proposed Eq. (8), which represents C_R for prediction of NF pulse-like IDR. This equation consists of exponential and logarithmic functions, which make it somehow sophisticated. Although this relationship estimates response of SDOF systems undergoing NF earthquakes with good accuracy, its complex form makes it less practical. Also, Iervolino *et al.* (2012) used bilinear hysteresis model with 3% post-elastic stiffness which differs from the model used here in this paper

$$C_R = 1 + \theta_1(T_P/T)^2.(R-1) + \theta_2.(T_P/T).\exp\left\{\theta_3.[\ln(T_P/T - 0.08)]^2\right\} + \\ + \theta_4.(T_P/T).\exp\left\{\theta_5.[\ln(T_P/T + 0.5 + 0.02.R)]^2\right\}$$

(8)

It appears that the polynomial form of expressions presented in this paper is more appropriate in practice. Another advantage of these equations is that they do not change the format of IDR in FEMA 440 and only modify the C_1 coefficient by multiplying a modification factor in order to consider NF effects. Also they allow the effects of various faulting mechanism to be taken into account. Moreover, C_R predicted by Eq. (7) is compared against those of Iervolino *et al.* (2012) in
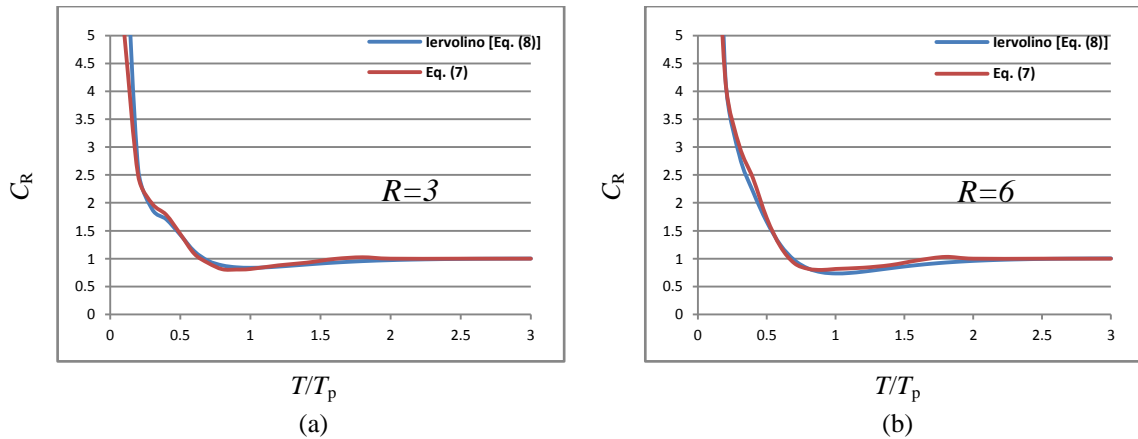

Fig. 10 Comparison of the mean IDRs for different *R* values vs. normalized period for all NF ground motions predicted by Eq. (7) and Eq. (8): (a) R=3, (b) R=6

Table 9 New NF ground motion ensemble for various fault types

#	Event	Year	Station	PGA	M_w	Closest D.	Soil Type	Fault Type
1	Loma Prieta	1989	Los Gatos - Lexington Dam	0.411	6.93	5.00	B	Reverse-Oblique
2	Northridge-01	1994	Pardee - SCE	0.557	6.69	5.54	C	Reverse
3	San Salvador	1986	National Geographical Inst.	0.404	5.80	3.71	C	Strike-Slip
4	Denali Alaska	2002	TAPS Pump Station #10	0.333	7.90	0.18	D	Strike-Slip
5	Loma Prieta	1989	Gilroy Array #3	0.367	6.93	12.23	D	Reverse-Oblique
6	Loma Prieta	1989	Saratoga - W Valley Coll.	0.331	6.93	8.48	D	Reverse-Oblique
7	Coyote Lake	1979	Gilroy Array #2	0.256	5.74	8.47	D	Strike-Slip
8	Coyote Lake	1979	Gilroy Array #3	0.256	5.74	6.75	D	Strike-Slip
9	Coyote Lake	1979	Gilroy Array #4	0.252	5.74	4.79	D	Strike-Slip
10	Northridge-01	1994	Pacoima Kagel Canyon	0.433	6.69	5.26	C	Reverse

Table 10 Calculated errors of 10 NF ground motions

Record #	Mean SRSS Error (%)				
	R=2	R=3	R=4	R=5	R=6
1	6.85	8.87	10.62	12.08	12.58
2	4.64	5.75	7.08	7.10	7.01
3	3.07	4.76	5.62	8.30	4.20
4	5.02	6.36	899	10.17	10.64
5	7.30	10.39	12.92	13.65	13.78
6	2.19	3.45	3.70	3.96	4.55
7	4.65	6.49	6.13	6.09	6.96
8	4.11	5.66	5.21	4.95	4.61
9	6.12	3.92	4.80	4.69	5.32
10	3.92	4.86	3.98	5.89	5.41

Fig. 10 at *R*=3 and *R*=6. This figure illustrates acceptable correspondence between the two Eq. (8) and the proposed equation of this paper.

In order to verify the degree of accuracy of Eq. (7), SDOF systems are subjected to some NF pulse-like ground motions that have not been used for deriving the proposed formulas. A total number of 10 NF ground motions, from 3 different aforementioned fault types are selected. The characteristic of these records are shown in Table 9.

The maximum displacement of each inelastic SDOF system was estimated using the NF modification factor (C_N) presented by Eq. (7). This inelastic displacement of each SDOF system was also computed using nonlinear response-history analyses. In order to measure the error of the proposed formula, the results of nonlinear response-history analyses are considered as the benchmark and the maximum displacements estimated using C_N are considered as the approximate ones.

An error measure is calculated for the data as the mean Square Root of the Sum of the Squares

(SRSS) of the normalized errors, as presented by Eq. (9), in which, *n* is the number of data points for each ground motions

$$\overline{E}_{SRSS} \ (\%) = \frac{1}{n} \sqrt{\sum_{i=1}^{n} \left[\frac{\left| (\Delta_i)_{app} - (\Delta_i)_{exact} \right|}{(\Delta_i)_{exact}} \times 100 \right]^2} \tag{9}$$

The results are shown in Table 10. They show that generally errors do not exceed 13% for most periods of vibration. The table also shows that for larger *R* ratios the mean of SRSS of error get larger.

In order to summarize the presented method of this paper, a flowchart is presented in Fig. 11, in which the steps of modification of DCM are considered in the way that the NF effects are included in determining the target displacements.
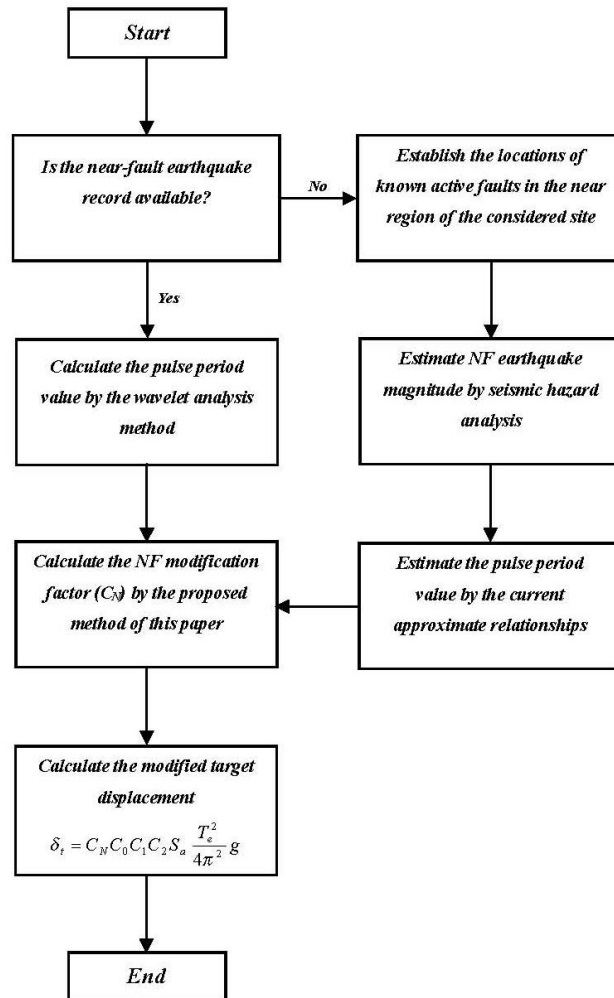
Fig.11. Flowchart of the modified displacement coefficient procedure considering NF effects

6. Conclusions

Nonlinear static procedures are vastly utilized as practical engineering methods in recent years, which can be appropriate substitutions of nonlinear dynamic procedures. The primary purpose of this paper was to assess IDRs that permit the estimation of maximum inelastic displacements from maximum elastic displacements for structures subjected to pulse-like NF ground motions. IDRs were computed for SDOF systems undergoing different levels of nonlinearity when subjected to a set of 96 NF records. For comparison, a set of 20 FF ground motions were also considered. The influences of different faulting mechanisms, including three main fault types, SS, DS and OS faults, were also investigated in this paper. The following conclusions can be drawn from the results of this study.

• The effects of NF earthquake ground motions on the response of structures are higher than FF earthquakes, in the whole region of periods.Limiting periods at which mean IDRs become equal to 1 depend on the level of inelastic deformation. Although these limiting periods increase with increasing strength ratios, equal displacement rule is applicable for periods longer than 3 s for NF strong motions.

• Various faulting mechanisms result into different values for the pulse period. Separate equations are presented here for various faulting mechanisms which estimate T_p by earthquake moment magnitude.

• The equal displacement rule is applicable for T/T_p ratios larger than about 0.6 for all strength ratios, regardless of their faulting mechanism. For smaller values of T/T_p, the equal displacement rule is not applicable as displacements ratios vary by R. For OS faults, this limiting ratio of T/T_p is about 0.65.

• Considerable differences in nonlinear seismic demand are obvious for various faulting mechanisms which demonstrate the fact that this parameter can have considerable influences on nonlinear response of structures. The results demonstrate that OS fault typecan cause larger demands compared to SS and DS fault types.

• The coefficient C_1 used in displacement coefficient method of FEMA 440 underestimates the NF ground motion responses in T/T_p<0.6 range and it overestimates the results in 0.6<T/T_p<2.0 range. Therefore, a NF modification factor, C_N, is presented in this paper. Polynomial functions of order 4 and 5 have been found to be able to estimate this modification coefficient for T/T_p<0.6 and 0.6<T/T_p<2.0, respectively. It appears that the proposed polynomial form of expressions is more appropriate in practice. Moreover, these equations do not change the format of IDR in FEMA 440 and only modifies the C_1coefficient by multiplying a modification factor in order to consider NF effects. Also they allow the effects of various faulting mechanism to be taken into account

• Despite the advantages of the proposed method in estimating inelastic displacement demand of SDOF structures subjected to NF ground motions, supplementory studies are required to extend it to other available NSPs, such as Capacity Spectrum Method (CSM), for which the NF effects are not considered in relevant codes yet.

• It must be emphasized that the EPP model considered in this paper has been widely used in previous investigations and therefore it represents a benchmark to study nonlinear behavior of structures. Therefore, the results presented here are only accurate for EPP models and similar analyses should be carried out using other hysteretic models to generalize the results.

References

Akkar, S.D., Yazgan, U. and Gulkan, P. (2004), "Deformation limits for simple non-degrading systems subjected to near-fault ground motions", *Proceedings of the Thirteen World Conference on Earthquake Engineering*, Vancouver, British Columbia, Canada.

ASCE 41-06 Standard (2007), "Seismic Rehabilitation of existing buildings", *American society of civil engineers*, US.

ATC-40 (1996), *Seismic Evaluation and Retrofit of Concrete Buildings*, ATC-40 Report, Applied Technology Council, Redwood City, California.

Baez, J.I. and Miranda, E. (2000), "Amplification factors to estimate inelastic displacement demands for the design of structures in the near field", *Proceedings of the 12th World Conference on Earthquake Engineering*, New Zealand Society for Earthquake Engineering, Upper Hutt, New Zealand.

Baker, J.W. (2008), "Identification of near-fault velocity pulses and prediction of resulting response spectra", *Geotechnical Earthquake Engineering and Soil Dynamics IV*, Sacramento, California.

Baker, J.W. (2007), "Quantitative classification of near-fault ground motions using wavelet analysis", *Bull. Seismol. Soc. Am.*, **97**(5), 1486-1501.

Behmanesh, I. and Khoshnudian, F. (2008), "Effect of soil-structure-interaction on inelastic displacement ratios of existing structures", *14th World Conference on Earthquake Engineering*, October 12-17, Beijing, China.

Chioccarelli, E. and Iervolino, I. (2010), "Near-source seismic demand and pulse-like records: A discussion for L'Aquila earthquake", *Earthq. Eng. Struct. Dyn.*, **39**(9), 1039-1062.

Clough, R.W. and Penzien, J. (2003), *Dynamics of structures, Third edition book*, Computers & Structures, Inc. Berkeley, USA.

Decanini, L.D., Liberatore, L. and Mollaioli, F. (2003), "Characterization of displacement demand for elastic and inelastic SDOF systems", *Soil Dyn. Earthq. Eng.*, **23**(6), 455-471.

Dimakopoulou, V., Fragiadakis, M. and Spyrakosl, C. (2013), "Influence of modeling parameters on the response of degrading systems to near-field ground motions", *Eng. Struct.*, **53**, 10-24.

Enderami, S.A., Beheshti-Aval, S.B. and Saadeghvaziri, M.A. (2014), "New energy based approach to predict seismic demands of steel moment resisting frames subjected to near-fault ground motions", *Eng. Struct.*, **72**, 182-192.

FEMA 273 Report (1997), *Building Seismic Safety Council*. NEHRP Guidelines for the Seismic Rehabilitation of Buildings, FEMA-273. Federal Emergency Management Agency, Washington, DC., US.

FEMA 356 Report (2000), *Prestandard and Commentary for the Seismic Rehabilitation of Buildings*, prepared by the American Society of Civil Engineers for the Federal Emergency Management Agency, Washington, DC., US.

FEMA 440 Report (2005), *Federal Emergency Management Agency*, Improvement of nonlinear static seismic analysis procedures, Washington, DC., US.

Hatzigeorgiou, G.D. and Beskos, D.E. (2008), "Inelastic displacement ratios for SDOF structures subjected to repeated earthquakes", *J. Eng. Struct.*, **31**(11), 2744-2755.

Iervolino, I., Chioccarelli, E. and Baltzopoulos, G. (2012), "Inelastic displacement ratio of near-source pulse-like ground motions", *Earthq. Eng. Struct. Dyn.*, **41**(15), 2351-2357.

Iwan, W.D., Huang, C.T. and Guyader, A.C. (2000), "Important features of the response of inelastic structures to near-field ground motion", *Proceedings of the 12th World Conference on Earthquake Engineering*, New Zealand Society for Earthquake Engineering, Upper Hutt, New Zealand.

Khoshnoudian, F., Ahmadi, E. and Abedi Nik, F. (2013), "Inelastic displacement ratios for soil-structure systems", *J. Eng. Struct.*, **57**, 453-464.

Ma, S. and Archulet, J.A. (2006), "Radiated seismic energy based on dynamic rupture models of faulting", *J. Geophys. Res.*, **111**, B05315.

MacRae, G. and Tagawa, H. (2001), "Methods to estimate displacements of PG&E structures", *draft report on research conducted under PGE/PEER Task No. 505*, University of Washington, Seattle, Washington,

DC.

Miranda, E. (2000), "Inelastic displacement ratios for displacement-based earthquake resistant design", *Proceedings of the 12th World Conference on Earthquake Engineering*, Auckland, New Zealand.

Miranda, E. (2000), "Inelastic displacement ratios for structures on firm sites", *J. Struct. Eng.*, **126**(10), 1150-1159.

Movahed, H., Meshkat-Dini, A. and Tehranizadeh, M. (2014), "Seismic evaluation of steel special moment resisting frames affected by pulse type ground motions", *Asian J. Civ. Eng.*, BHRC, **15**(4), 575-585.

Ozkul, S., Ayoub, A. and Altunkaynak, A. (2014), "Fuzzy-logic based inelastic displacement ratios of degrading RC structures", *J. Eng. Struct.*, **75**, 590-603.

Ruiz-Garcìa, J. (2011), "Inelastic displacement ratios for seismic assessment of structures subjected to forward-directivity near-fault ground motions", *J. Earthq. Eng.*, **15**(3), 449-468.

Ruiz-Garcìa, J. and Miranda, E. (2006), "Inelastic displacement ratios for evaluation of structures built on soft soil sites", *Earthq. Eng. Struct. Dyn.*, **35**(6), 679-694.

Ruiz-Garcìa, J. and Miranda, E. (2012), "Evaluation of seismic displacement demands from ground motions recorded in recent earthquakes", *15th World Conference on Earthquake Engineering*, Lisbon, Portugal.

Shahi, S.K. and Baker, J.W. (2011), "Regression models for predicting the probability of near-fault earthquake ground motion pulses, and their period", *11th International Conference on Applications of Statistics and Probability in Civil Engineering*, Zurich, Switzerland.

Shaw, R. and Goda, K. (2004), "From disaster to sustainable civil society: The Kobe experience", *Disasters*, **28**(1), 16-40.

Wen, W.P., Zhai, C.H., Li, S., Chang, Z. and Xie, L.L. (2014), "Constant damage inelastic displacement ratios for the near-fault pulse-like ground motions", *Eng. Struct.*, **59**, 599-607.

Zhai, C.H., Wena, W.P., Zhu, T.T., Li, S. and Xie, L.L. (2013), "Inelastic displacement ratios for design of structures with constant damage performance", *Eng. Struct.*, **52**, 53-63.

Ruiz-Garcìa, J. and Gonzalez, E.J. (2014), "Implementation of displacement coefficient method for seismic assessment of buildings built on soft soil sites", *J. Eng. Struct.*, **59**, 1-12.

CC